# Synthesis of Diazocine-Containing Poly(arylene ether sulfone)s for Tailored Mechanical and Electrochemical Performance

**Takeo Suga, Sungsool Wi, and Timothy E. Long***

*Department of Chemistry, Virginia Tech, Blacksburg, Virginia 24061*

*Received October 8, 2008; Revised Manuscript Received January 14, 2009*

ABSTRACT: A series of poly(arylene ether sulfone) copolymers containing the diazocine unit (0, 20, 50, 80, 100 mol %) were synthesized *via* step-growth polymerization. Copolymer compositions exhibited number-average molecular weights exceeding 30 000 g/mol, and mechanically ductile films were obtained for all compositions. The random copolymers exhibited enhanced thermal stability ($T_{d10\%}$ = 500−550 °C) and mechanical properties (tensile stress = 45−65 MPa), and the thermomechanical performance was predictable based on copolymer composition. A secondary transition in the dynamic mechanical analysis appeared at 28 °C, which was attributed to segmental motion of the bulky diazocine and biphenyl units. X-ray single crystallography and $^1$H NMR spectroscopy as a function of temperature revealed that the diazocine ring existed in the boat-shaped conformation. The effective dipolar couplings of site-specific $^1$H−$^{13}$C dipolar couplings in the aromatic rings were measured using DIPSHIFT solid state NMR spectroscopy at various temperatures. The experimental data indicated that the bulkier diazocine group experienced slower ring-flip motion than the smaller phenylene group. Cyclic voltammograms of diazocine-containing poly(arylene ether sulfone)s exhibited two reversible reduction peaks at −0.68 and −1.21 V under inert and basic conditions. UV spectra of the diazocine group in the reduced state indicated an extended $\pi$-electron structure, which supported the boat- to planar-conformational change (molecular actuation) *via* redox reactions.

## Introduction

Poly(arylene ether)s and poly(arylene ether sulfone)s are commonly regarded as high performance engineering thermoplastics with excellent thermal stability, desirable mechanical properties, and acceptable resistance to hydrolysis and oxidation. Thus, polysulfones have attracted significant interest as insulating materials in microelectronics and as membrane materials for gas separation, water purification and proton conduction.[1,2] Recent focus has been placed on solution-processability, enhanced toughness, and improved thermal stability of poly(arylene ether sulfone)s with relatively high glass transition temperatures. For example, poly(biphenylsulfone) is commercially available as Radel-R (Solvay Advanced Polymers), and offers a relatively high impact strength and glass transition temperature ($T_g$ = 220 °C), which enable many aerospace, automotive, and biomedical applications.

Extensive research on the dynamic mechanical behavior of systematically modified poly(arylene ether sulfone)s has been employed to understand structure−property relationships, however, the correlation of high impact strength and chemical structure remains challenging.[3−7] Earlier research efforts attempted to correlate dynamic mechanical behavior and local chain motion of polycarbonate glasses. Sub-$T_g$ relaxation processes (*e.g.*, $\beta$- or $\gamma$-transition) were proposed to involve cooperative motion of several units that alter the local volume or shape of the glass resulting in rapid decreases in stress concentration. Earlier work has also revealed that phenylene ring $\pi$ flips are sensitive to local, mechanically active volume-fluctuations in the glass. Thus, intermolecular chain packing or free volume strongly affects sub-$T_g$ behavior.[8−11]

In this work, we focus on the incorporation of nonplanar hetero[8]annulene, diazocine, which provides dynamic segmental motion resulting from its bulky nature and unique conformational characteristics, and diazocine-containing poly(arylene ether sulfone)s are hypothesized to enhance and tune mechanical performance. Poly(arylene ether sulfone)s are generally prepared via a step-growth polymerization of activated aryl dihalo monomers with bisphenolate salts, resulting in high molecular weight polymers with controlled copolymer composition *via* judicious selection of monomer stoichiometry.[12−19] Moreover, the diazocine group serves as a cyclotetraene analog, which has a nonplanar 8-membered ring structure with two nitrogen atoms, and diazocine units are expected to exhibit the boat- (neutral state) to planar- (dianion) conformational change *via* a two electron transfer process (Scheme 1).[20−22] This dynamic conformational change at the molecular level, which utilizes chemical, electrochemical, or photochemical stimulation, has also attracted significant interest as a basis for molecular machines.[23−27] Marsella, et al. have reported redox-induced conformational changes of the cyclooctatetraene unit, such as thiophene-fused[8] annulene, and proposed a potential electromechanical actuators.[28,29] Herein, we report the conformational analysis of a diazocine derivative, 6,12-bis(4-fluorophenyl)dibenzo[1,5]diazocine **1**, *via* $^1$H NMR spectroscopy and X-ray single crystallography, and we also report the unprecedented synthesis of high glass transition temperature diazocine-containing poly(arylene ether sulfone)s **4**. The thermomechanical, tensile, and electrochemical properties of these novel copolymers are also described.

## Experimental Section

**Materials.** Solvay Advanced Polymers provided 6,12-bis(4-fluorophenyl)dibenzo[1,5]diazocine (**1**), biphenol, and anhydrous $K_2CO_3$. The diazocine monomer was recrystallized from chloroform/hexane (1/4 v/v) to ensure high purity. Di(4-fluorophenyl)sulfone was purchased from Aldrich Chemical Co. and used as received without further purification.

**Scheme 1. Boat to Planar Conformational Change of Diazocine via a Two-Electron Transfer Process**

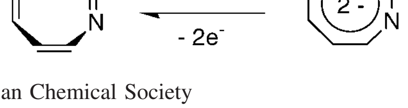

---

[*] To whom correspondence should be addressed. Telephone: 540-231-2480. E-mail: telong@vt.edu.

10.1021/ma802249a CCC: $40.75

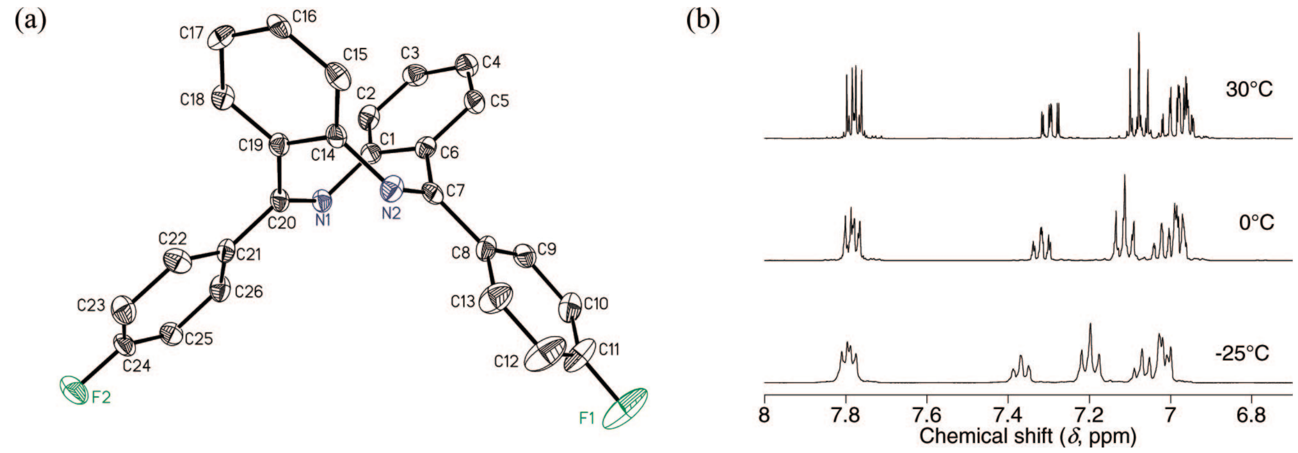

**Figure 1.** (a) ORTEP view of 6,12-bis(4-fluorophenyl)-dibenzo-[1,5]diazocine (**1**) with hydrogen atoms removed. (b) $^1$H NMR spectra of **1** in THF-$d_8$ at various temperatures.

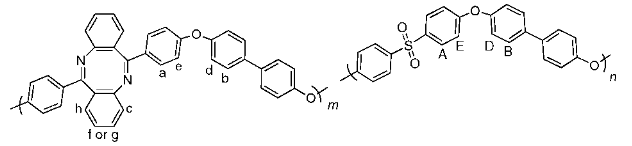

**4a-d**

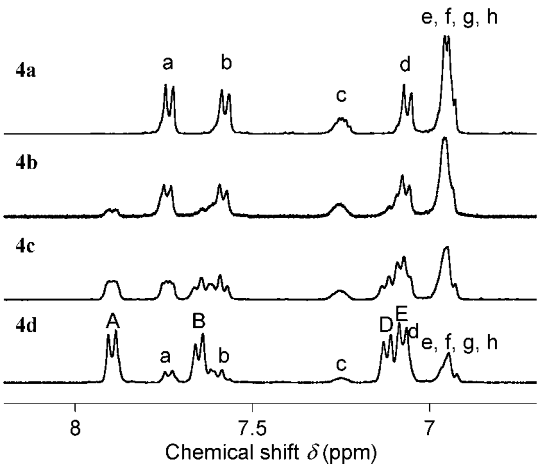

**Figure 2.** $^1$H NMR spectra of diazocine-containing poly(arylene ether sulfone) copolymers in THF-$d_8$: (a) **4a** (diazocine/sulfone 1.0/0); (b) **4b** (0.81/0.19); (c) **4c** (0.50/0.50); (d) **4d** (0.20/0.80). Poly(biphenylsulfone) **4e** was not shown above due to its insolubility in THF.

**Synthesis of Diazocine-Containing Poly(arylene ether) (4a).** 6,12-Bis(4-fluorophenyl)dibenzo[1,5]diazocine (**1**) (5.17 g, 13.1 mmol), biphenol **2** (2.38 g, 13.1 mmol), anhydrous $K_2CO_3$ (2.12 g, 15.3 mmol), and anhydrous *N,N*-dimethylacetamide (DMAc, 37 mL) were added into a 100-mL, three-necked round-bottomed, flask at approximately 20 wt % solids in DMAc. Approximately 50 vol % dry toluene (18 mL), based on DMAc, was used as a dehydrating agent. The reaction apparatus was equipped with an overhead mechanical stirrer, a dry nitrogen inlet, and a Dean−Stark trap attached to a reflux condenser. The reactor was carefully purged with nitrogen and the reaction was performed at 135 °C for 12 h to complete dehydration (removal of the residual water by azeotropic reflux with toluene). After the removal of water/toluene, the polymerization was performed at 155 °C for 24 h. The reaction solution was allowed to cool to ambient conditions and the reaction mixture was precipitated into methanol, washed with water, and finally dried at reduced pressure. The resulting powder was dissolved in THF and reprecipitated into methanol. The final powder product was completely dried under vacuum at 140 °C for 48 h (yield 98%). $M_n$(SEC) = $3.41 \times 10^4$, $M_w/M_n = 1.81$. $^1$H NMR (THF-$d_8$, 400 MHz, ppm): $\delta$ = 7.73 (d, 4H, Ph), 7.58 (d, 4H, biphenyl CH), 7.24 (m, 2H, benzo CH), 7.06 (d, 4H, biphenyl CH), 7.0−6.6 (br, 4H (Ph) + 6H (benzo CH)). $^{13}$C NMR ($CDCl_3$, 125 MHz, ppm): $\delta$ = 169.7, 161.8, 157.6, 154.1, 137.9, 134.7, 132.8, 131.1, 129.9, 129.1, 128.5, 124.7, 122.5, 121.4, 119.4. IR (cm$^{-1}$): 2922 ($\nu_{PhC-H}$), 1620 ($\nu_{C=N}$), 1231 ($\nu_{Ph-O}$), 960, 853 ($\nu_{diazocine}$).

**Synthesis of Poly(arylene ether sulfone) Copolymer Containing Diazocine 4d (20 mol %).** The polymerization procedure was identical to that used to obtain **4a**. 6,12-Bis(4-fluorophenyl)-dibenzo[1,5]diazocine (**1**) (0.847 g, 2.15 mmol), di(4-fluorophenyl)sulfone (**2**) (2.21 g, 9.01 mmol), biphenol **3** (2.00 g, 10.74 mmol), 4-*tert*-butylphenol (32.2 mg, 0.214 mmol), anhydrous $K_2CO_3$ (1.86 g, 13.4 mmol), and anhydrous *N,N*-dimethylacetamide (DMAc, 25 mL) were added into a 100-mL, three-necked, round-bottomed flask at approximately 20 wt % solids in DMAc. Approximately 50 vol % dry toluene (13 mL) based on DMAc was used as a dehydrating agent. After dehydration at 135 °C (12 h) and polymerization at 155 °C (24 h), the reaction mixture was precipitated into methanol, washed with water, and dried at reduced pressure. The obtained powder was dissolved in THF and reprecipitated into methanol. The resulting polymer powder was quantitatively dried under vacuum at 140 °C for 48 h (yield 99%). $M_n = 2.72 \times 10^4$, $M_w/M_n = 2.44$. $^1$H NMR (THF-$d_8$, 400 MHz, ppm): $\delta$ = 7.91 (d, 4H, Ph), 7.76 (d, 1H, diazocine Ph), 7.67 (d, 4H, Ph), 7.61 (d, 1H, biphenyl CH), 7.27 (m, 0.5H, benzo CH), 7.14 (d, 4H, Ph), 7.09 (d, 4H (Ph) + 1H (biphenyl CH)), 7.0−6.95 (br, 1H (Ph) + 1.5H (benzo CH)); $^{13}$C NMR ($CDCl_3$, 125 MHz, ppm): $\delta$ = 166.6, 162.2, 160.6, 156.6, 155.4, 152.8, 137.4, 137.3, 136.7, 133.6, 131.6, 130.4, 129.9, 129.2, 128.7, 127.8, 127.3, 123.5, 121.2, 121.0, 120.1, 118.3, 118.2; FTIR (cm$^{-1}$): 2922 ($\nu_{PhC-H}$), 1620 ($\nu_{C=N}$), 1294, 1147 ($\nu_{>S=O_2}$), 1231 ($\nu_{Ph-O}$), 960, 853 ($\nu_{diazocine}$).

**Characterization.** $^1$H, $^{13}$C, and 2D NMR (COSY, HSQC, and HMBC) spectra were collected in THF-$d_8$ or DMF-$d_7$ on a Varian INOVA 400 MHz spectrometer at ambient temperature or the controlled temperature. X-ray single crystallographic analysis was performed on Oxford Diffraction Gemini diffractometer operating with Mo radiation and equipped with a Sapphire 3 CCD detector. The data collection routine, unit cell refinement, and data processing were performed with the CrysAlis program. Size exclusion chromatography (SEC) was performed at 40 °C in HPLC grade tetrahydrofuran at 1 mL/min using a Waters size-exclusion chromatographer equipped with an autosampler, 3 in-line 5 mm PLgel MIXED-C columns. Detectors included a Waters 410 differential refractive index (DRI) detector operating at 880 nm, and a Wyatt Technologies miniDAWN multiangle 690 nm laser light scattering (MALLS) detector, calibrated with PS standards. All reported molecular weight values are absolute molecular weights obtained using SEC-MALLS detector. Thermal stability was measured with a TA Instruments Hi-Res Thermogravimetric Analyzer 2950, with a temperature ramp of 10 °C/min under nitrogen atmosphere. Differential scanning calorimetry (DSC) was performed on a TA

**Scheme 2. Synthesis of Diazocine-Containing Poly(arylene ether sulfone) Copolymers**

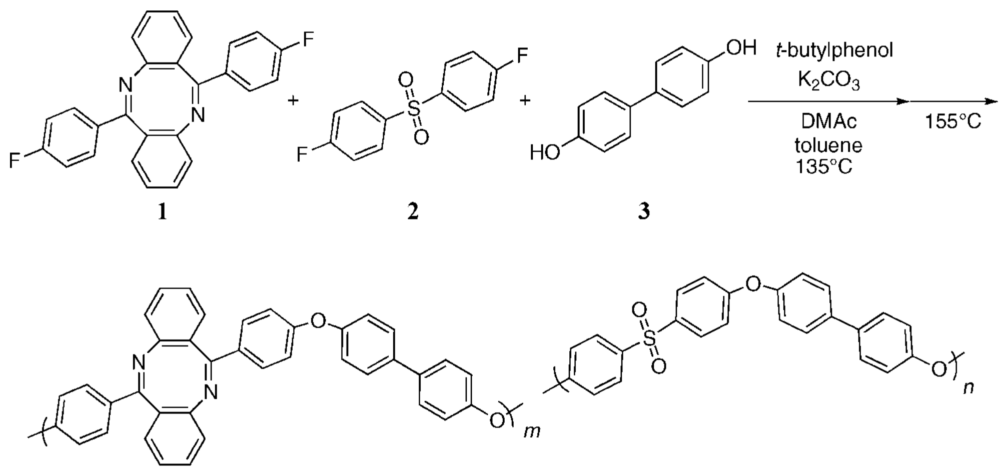

**1** **2** **3**

**4a-e**

**Table 1. Polymerization Conditions and Characterization**

| | feed ratio (**1**/**2**/**3**) | composition (**1**/**2**) | $M_n$ | $M_n{}^b$ | $M_w/M_n$ | $T_{d10\%}$ (°C) | $T_g$ (°C) | yield (%) |
|---|---|---|---|---|---|---|---|---|
| **4a** | 1/0/1.001 | 1/0 | 34 100 | | 1.81 | 557 | 309 | 98 |
| **4b**[a] | 0.81/0.2/1.00 | 0.81/0.19 | 31 200 | 45 100 | 2.07 | 537 | 291 | 97 |
| **4c** | 1/1.001/2.007 | 0.50/0.50 | 49 800 | | 1.81 | 515 | 276 | 89 |
| **4d**[a] | 0.2/0.81/1.00 | 0.20/0.80 | 27 200 | 35 300 | 2.44 | 514 | 250 | 99 |
| **4e**[a] | 0/1.01/1.00 | 0/1 | 40 900[c] | 37 300 | 1.62[c] | 502 | 230 | 97 |

[a] End capped with *tert*-butylphenol. [b] $M_n$ was calculated from $^1$H NMR spectroscopic analysis of the end group. [c] DMF as an eluent for SEC characterization.

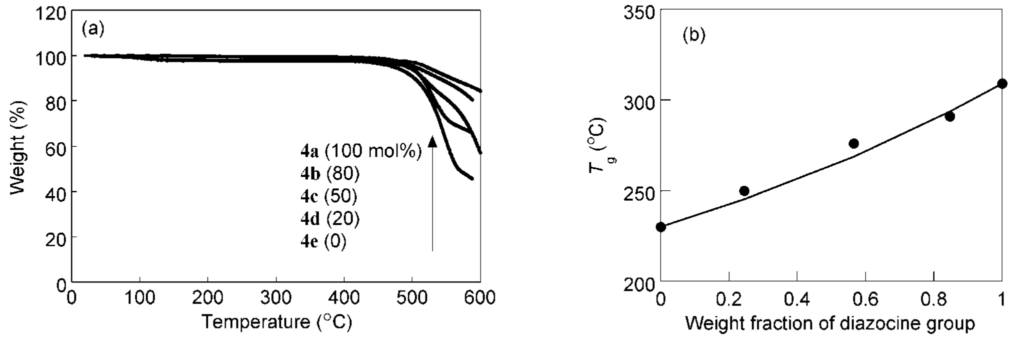

**Figure 3.** (a) Thermogravimetric analysis (TGA) of diazocine-containing poly(arylene ether sulfone) copolymers **4a**−**4e**. (b) Glass transition temperature vs weight fraction of the diazocine group. Solid line was drawn according to the Fox equation.

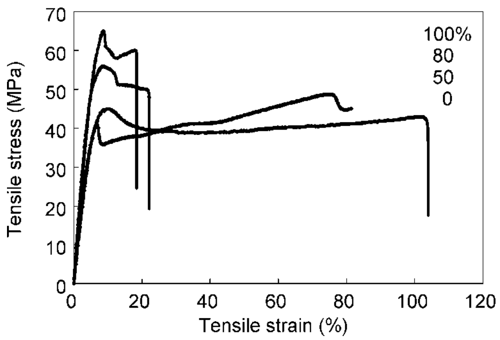

**Figure 4.** Stress−strain curves for diazocine-containing poly(arylene ether sulfone) copolymers, deformation rate = 0.02 min$^{-1}$.

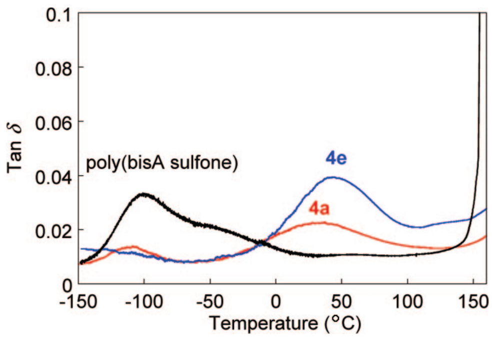

**Figure 5.** Dynamic mechanical analysis of (a) poly(bis-A-phenylsulfone), (b) poly(biphenylsulfone) **4e**, and (c) diazocine-containing poly(arylene ether) **4a**.

Instruments DSC Q1000 under a nitrogen flush at a heating rate of 10 °C/min. $T_g$ was calculated from the second heat using the midpoint method. Dynamic mechanical analysis (DMA) measurements were performed on a TA Instruments Q-800 DMA under nitrogen at a heating rate of 3 °C/min, an oscillatory amplitude of 15 $\mu$m at 1 Hz frequency. The samples were measured in film tension mode, on solvent cast samples. Stress−strain experiments were performed with dog bone-shaped film specimens, cut with a die according to ASTM D3368 specifications. Tensile tests were conducted on an Instron 4411 universal testing instrument with a crosshead speed of 0.02 min$^{-1}$ using manual grips at ambient temperature.

**Solid-State NMR Spectroscopy.** Cross-polarization magic-angle spinning (CPMAS) $^{13}$C NMR spectra of the diazocine-containing polysulfones were obtained on a Bruker Avance II 300 MHz

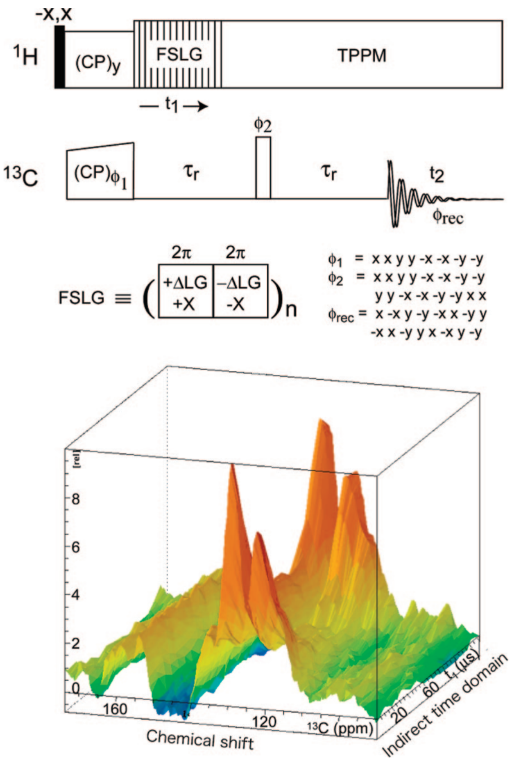

**Figure 6.** Pulse sequence and separated local field (SLF) $^{13}$C NMR spectra of poly(arylene ether) containing the diazocine group (100 mol %) as a function of the $^1$H−$^{13}$C dipolar evolution time.

spectrometer operating at the resonance frequencies of 300.21 MHz for $^1$H, and 75.47 MHz for $^{13}$C, using a Bruker 4.0 mm MAS NMR probe. Cross-polarization for 1 ms mixing time was achieved at 50 kHz *rf*-field at the $^1$H channel and linearly ramping the $^{13}$C *rf*-field over a 25% range centered at 38 kHz. A separated local field (SLF) NMR experiment,[30−32] which is also named a dipolar shift (DIPSHIFT) correlation experiment (Figure 6), was performed to investigate the ring-flip segmental motion of aromatic rings in the polymer main chain by measuring the site-specific one-bond $^1$H−$^{13}$C dipolar couplings in the aromatic rings. A conventional two-dimensional (2D) DIPSHIFT correlation scheme was incorporated to encode site-specific $^1$H−$^{13}$C dipolar couplings indirectly while acquiring $^{13}$C CPMAS spectra directly at the spinning speed $\nu_r$ = 4242 Hz. Carbon magnetization after CP is allowed to evolve during a variable time $t_1$ under the influence of $^{13}$C chemical shift and $^1$H−$^{13}$C dipolar coupling interaction, while the $^1$H−$^1$H homonuclear dipolar coupling is suppressed by $^1$H irradiation implemented in a frequency-switched Lee-Goldburg (FSLG) scheme.[33] The maximum FSLG ($\nu_{rf}$(LG) = 97 kHz; offset frequency = ± 68.6 kHz) period during $t_1$ was one rotor period (= 235.7 $\mu$s), which is 14 times a $t_1$ increment that corresponds to a basic FSLG unit, $(8.42\ \mu s)_0(8.42\ \mu s)_{180}$, where 0 and 180 designate the *rf*-pulse phase (in degrees) of FSLG decoupling pulse irradiation. The $^{13}$C Hahn echo signal at $t_2$ = 0 removes the effect of chemical shift and leaves the $^1$H−$^{13}$C dipolar coupling as the only effective interaction during the evolution time $t_1$. The $t_1$-dependent modulation of the resulting line intensities in the spectra were used to extract the effective $^1$H−$^{13}$C dipolar coupling strength that is under the influence of the fast ring-flip dynamic process of an aromatic ring. A total of 2048 transient signals were accumulated under 63 kHz of two-pulse phase modulated (TPPM) proton decoupling[34] during signal acquisition with acquisition delay for 4 s on 50−60 mg of samples. By monitoring with a thermocouple situated near the sample coil, the temperature of the sample compartment during NMR measurements was maintained at 20 and 65 °C with air flow from the BCU-X temperature control unit.

**Electrochemical Measurement.** Cyclic voltammetry was performed using a normal potentiostat system (CH Instruments, Inc., CHI620B) with a conventional three-electrode cell under a dry nitrogen atmosphere. A platinum disk, platinum wire, and Ag/Ag$^+$ were used as the working, auxiliary and reference electrode, respectively. The cyclic voltammograms was measured in a 1.0 mM tetrahydrofuran solution of diazocine **1** and polymer **4a** in the presence of 0.1 M tetrabutylammonium perchlorate as the supporting electrolyte. The methanolic solution of tetrabutylammonium hydroxide was used as the organic base additive. The formal potential of the ferrocene/ferrocenium redox couple was 0.45 V vs Ag/Ag$^+$ reference electrode. Cyclic voltammogram of the film **4a** on the ITO electrode (thickness ∼ 80 nm) was measured in acetonitrile/THF (9/1) solution in the presence of 0.1 M tetrabutylammonium perchlorate and tetrabutylammonium hydroxide.

## Results and Discussion

**Conformation of the Diazocine Monomer.** Recrystallization of the diazocine monomer, 6,12-bis(4-fluorophenyl)-dibenzo-[1,5]diazocine **1**, from chloroform/hexane (1/4 v/v) solution provided a light yellow crystal. X-ray crystallographic analysis of the single crystal **1** exhibited monoclinic (space group: $P2_1/c$; $a$ = 18.090(2) Å, $b$ = 20.368(2) Å, $c$ = 16.6509(15) Å; α = 90°, $\beta$ = 104.245(11)°, $\gamma$ = 90°) and proved the boat-conformation of the 8-membered ring with alternating bond lengths (Figure 1a and Supporting Information). Nonplanarity of the 8-membered ring minimizes the delocalization of the double bonds and prevents antiaromaticity. The proton peaks in $^1$H NMR spectra for **1** broadened with decreasing temperatures (30 to −25 °C) due to the slow relaxation time, however, no additional peaks corresponding to another conformation appeared in this temperature range (Figure 1b). On the basis of these two analyses, the ground-state of **1** was identified as the boat-conformation.

**Polysulfone Synthesis.** Diazocine-containing poly(arylene ether) and poly(arylene ether sulfone) copolymers were synthesized from 6,12-bis(4-fluorophenyl)-dibenzo[1,5]diazocine (**1**), di(4-fluorophenyl)sulfone (**2**), and biphenol **3** *via* step-growth polymerization (Scheme 2). The resulting copolymers exhibited a yellow color attributed to the diazocine unit. The compositional molar ratios of the diazocine group (0, 20, 50, 80 and 100 mol %) in the poly(arylene ether sulfone) copolymers were controlled stoichiometrically with the feed ratio of the corresponding difluoro monomers (Figure 2). The copolymers were also end capped with *tert*-butylphenol for molecular weight determination. SEC and end group analysis using the integrations from the $^1$H NMR spectrum estimated the number-average molecular weight ($M_n$) of the polymeric products (Table 1). While the solubility of poly(biphenylsulfone) **4e** (diazocine 0%) was limited in aprotic polar solvents such as DMAc, *N,N*-dimethylformamide (DMF), and *N*-methyl-2-pyrrolidone (NMP), the obtained poly(arylene ether sulfone) containing diazocine group **4a−d** showed solubility in THF even with 20 mol % diazocine incorporation.

The diazocine-containing copolymers exhibited enhanced thermal stability ($T_{d10\%}$ > 500 °C). The glass transition temperatures ($T_g$) for poly(arylene ether sulfone) copolymers also increased with diazocine content, which was attributed to the retardation of segmental motion by the bulky group substitution. The change in $T_g$ adhered to the Fox equation: ($T_g^{-1}$ = $w_1/T_{g1} + w_2/T_{g2}$, where $w$ is weight fraction, and $T_{g1}$ and $T_{g2}$ are the glass transition temperatures of each homopolymers), which suggested a random copolymer composition and equal reactivity of monomers **1** and **2** (Table 1, Figure 3b).

**Mechanical Properties.** All films were prepared via solution casting from a homogeneous THF solution, and dried at 150 °C for 96 h in vacuo. Conventional tensile testing of a series of diazocine-containing polysulfone copolymers (diazocine content: 50, 80, and 100%) revealed high Young's moduli (*ca.* 1400

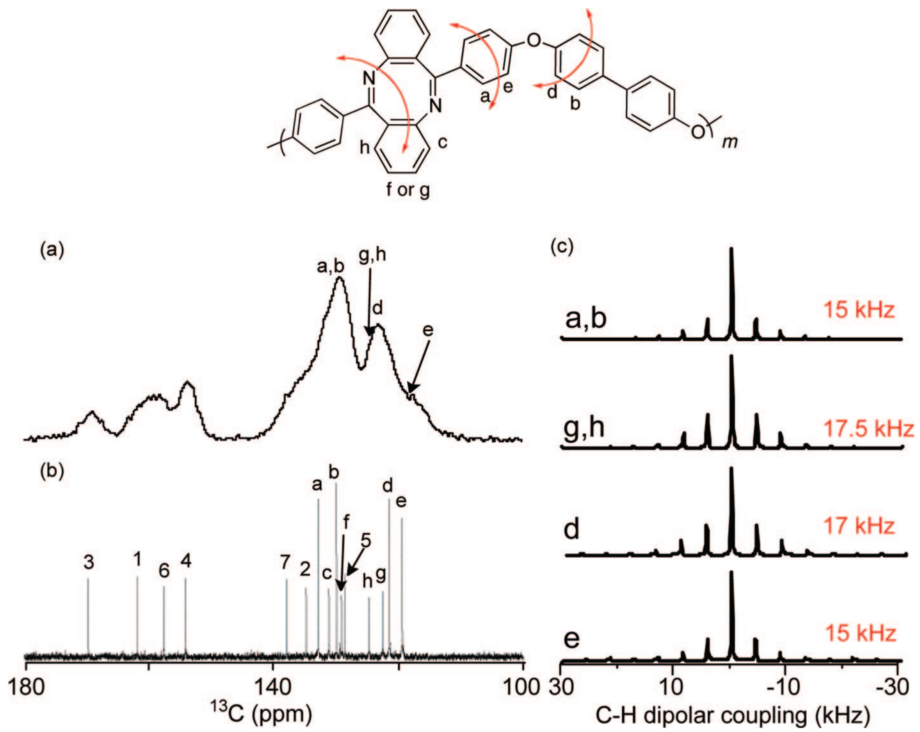

**Figure 7.** (a) $^{13}$C cross polarization magic-angle spinning (CPMAS) NMR spectrum projected along the direct time domain of 2D DIPSHIFT spectrum (Figure 6), and (b) solution $^{13}$C NMR spectrum measured on the polysulfone containing diazocine 100 mol %, **4a**. Peaks were precisely assigned based on 2D solution NMR spectra (see Supporting Information). (c) Site-specific $^1$H−$^{13}$C dipolar sideband patterns obtained. $^1$H−$^{13}$C dipolar coupling strengths were obtained based on the best-fit simulation spectra.

**Table 2. $^{13}$C−$^1$H Dipolar Coupling (Hz)**

| | | diazocine benzo (*g*, *h*) | | diazocine phenyl (*a*, *e*) | | sulfone phenyl (*A*, *E*) | | biphenyl (*b*) | |
|---|---|---|---|---|---|---|---|---|---|
| | diazocine (mol %) | 22 °C | 65 °C | 22 °C | 65 °C | 22 °C | 65 °C | 22 °C | 65 °C |
| **4a** | 100 | 17.5 | 17.5 | 15 | 15 | | | 15 | 15 |
| **4c** | 50 | 16 | 16 | 15 | 15 | | | 15 | 14.5 |
| **4e** | 0 | | | | | 15 | 14.5 | 15 | 14.5 |

MPa) and high tensile strengths at yield (*ca.* 45−65 MPa), which increased with diazocine content. Elongations at break of these films were 15−25% (Figure 4). These tensile results supported that the introduction of the diazocine unit contributed to increased moduli of the optically clear polysulfone films. In a small range of deformation (prior to yielding), the larger area under the tensile curves for diazocine-containing polysulfones suggested enhanced toughness resulting from diazocine incorporation.

Dynamic mechanical analysis was performed on the copolymer films (film thickness: 30−50 $\mu$m). Temperature sweeps from −150 to 300 °C at a constant frequency (1.0 Hz) and constant strain (0.2%), showed glass transitions (α-relaxation) above 200 °C, corresponding to the diazocine content in the copolymer. While poly(bis-A-sulfone) (UDEL) exhibited a secondary ($\gamma$-) transition at −100 °C, poly(biphenylsulfone) **4e** indicated a $\beta$-transition at 40 °C and a $\gamma$-transition at −140 °C. Poly(biphenylsulfone) is known to exhibit an order of magnitude higher impact performance compared to poly(bis-A-sulfone), which is attributed to the biphenyl unit.[35] Diazocine-containing poly(arylene ether) **4a** indicated a similar secondary relaxation behavior (28 °C for the $\beta$-transition and −120 °C for the $\gamma$-transition) as **4e**, which also suggested the possibility for high impact performance (Figure 5). The damping peak for $\beta$-transition of **4a** is slightly smaller than that of **4e**, however, the lower shift of the $\beta$-peak for **4a** indicated that $\beta$-relaxation was not as restricted as **4e**, due to the larger free volume of the diazocine unit. The peak shift of the $\beta$-transition at higher applied frequencies (1, 10, and 100 Hz) was indicative of a lower activation energy (87 kJ/mol) for **4a**, compared to 111 kJ/mol for **4e**, which also supported a contribution from larger local free volume of diazocine group (see Supporting Information).

**Local Chain Motion Investigated via Solid-State NMR Spectroscopy.** One-dimensional (1D) $^{13}$C CPMAS spectroscopy of homopolymers and copolymers containing 100 mol %, 50 mol %, and 0 mol % diazocine were performed to obtain site-specific $^{13}$C NMR spectra in solid state. As a typical example, $^{13}$C CPMAS spectrum of homopolymer **4a** was represented in Figure 7a. In addition, the solution $^{13}$C NMR spectrum measured in THF-$d_8$ is included for guiding complete peak assignments because of limited resolution of solid-state $^{13}$C CPMAS spectra (Figure 7b). In $^{13}$C CPMAS spectra, peaks assigned as *g*, *h* from the diazocine group, and *d* from biphenyl group are partially overlapping. Approximately, peak regions from 115−134 ppm and 134−165 ppm corresponded to aromatic secondary carbons containing C−H groups and aromatic quaternary carbons, respectively.

The effective dipolar couplings of site-specific $^1$H−$^{13}$C dipolar couplings of aromatic rings in copolymer samples were measured using 2D DIPSHIFT solid state NMR spectroscopy at 22 and 65 °C. The later condition corresponded to a temperature well above $\beta$-transition temperatures of the polymers. Figure 7a illustrates the projected 1D $^{13}$C spectrum obtained from the 2D DIPSHIFT spectrum measured on the sample containing 100 mol % diazocine. Figure 7c demonstrates the sideband patterns of $^1$H−$^{13}$C dipolar vectors taken at the four different frequencies assigned at (*a*, *b*), (*g*, *h*), *d*, and *e* sites along the

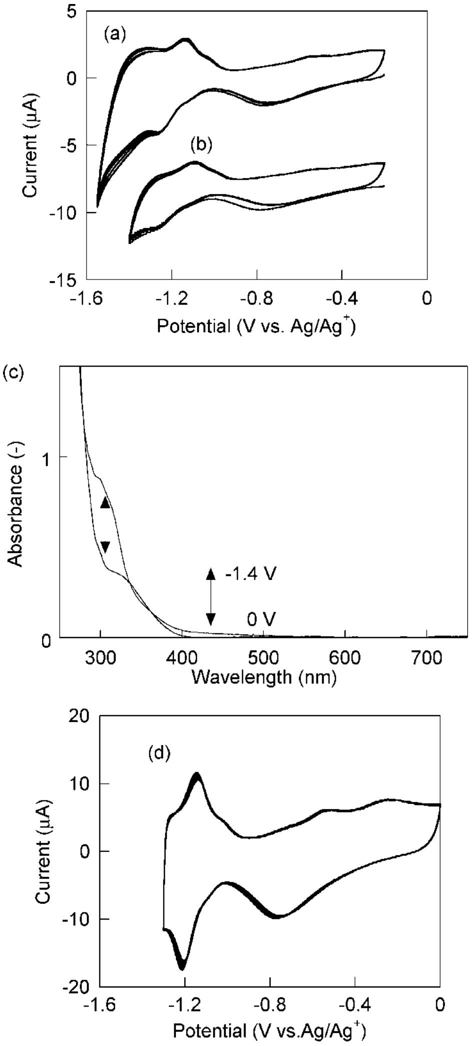

**Figure 8.** Cyclic voltammograms of (a) diazocine monomer **1** (1 mM) and (b) diazocine-containing poly(arylene ether) **4a** in 1 mM THF solution with 0.1 M $N(C_4H_9)_4ClO_4$ as the supporting electrolyte under basic condition, 100 mV/s, 5 cycles. $Fc/Fc^+ = 0.45$ V vs $Ag/Ag^+$. (c) UV−vis spectral change of **1** under an applied potential of −1.4 and 0 V. (d) Cyclic voltammogram of the film **4a** in the acetonitrile/THF (9/1) solution with 0.1 M $N(C_4H_9)_4ClO_4$ as the supporting electrolyte under basic condition, 10 mV/s, 10 cycles.

indirect time-domain $t_1$ of a 2D data set. A completely site-specific $^1H-^{13}C$ dipolar coupling measurement is limited by the insufficient spectral resolutions along the direct acquisition domain, particularly between *a* and *b* sites, and among *g*, *h* and *d* sites. The dipolar sideband pattern along the indirect time domain $t_1$ is obtained by the Fourier transformation of the time domain data set, which is constructed by concatenating 256 times the experimentally measured basic $t_1$ data points for one rotor period. The signal decay due to $T_2$ relaxation was corrected before the concatenation and a line broadening factor (50−80 Hz) was applied to the concatenated data set before the Fourier transformation. The dipolar sideband patterns thus obtained demonstrated the magnitudes of effective $^1H-^{13}C$ dipolar couplings of (*a*, *b*), (*g*, *h*), *d*, and *e* sites as demonstrated in Figure 7c. Also, Figure 7c depicts the magnitude of the effective $^1H-^{13}C$ dipolar coupling of the corresponding $^1H-^{13}C$ site based on the best-fit numerical simulation (theoretical simulation is shown in the Supporting Information). The effective $^1H-^{13}C$ dipolar coupling obtained along the overlapped peak site of (*g*, *h*) and *d* showed 17−17.5 kHz, while the effective $^1H-^{13}C$ couplings along the other two peak positions assigned as (*a*, *b*) and *e* were 15 kHz. As can be seen from the peak assignments shown in Figure 7, (*g, h*) sites originate from diazocine group and (*a*, *b*), *d*, and *e* all originate from phenylene group. These experimental data indicated that the bulkier diazocine group undergoes relatively slower ring-flip motion compared to the smaller phenylene group. This result is reasonable in the sense that the bigger diazocine group would be less favorable than the smaller phenylene group for a segmental, ring-flip motion.

We also performed DIPSHIFT experiments at a temperature above the $\beta$-transition temperatures of the copolymers (65 °C). We observed that the biphenyl group showed increased ring-flip mobility (decreased effective $^1H-^{13}C$ coupling strength) under elevated temperature above the $\beta$-transition, however, the segmental mobility of the diazocine group remained at the value observed below the $\beta$-transition temperature. This fact indicated that the segmental mobility of biphenyl group was mainly under the influence of the structural relaxation due to the $\beta$-transition. In addition, we can conclude that, generally, the biphenyl group possesses higher mobility and lower activation energy for local motion than the larger diazocine group at below and above the $\beta$-transition temperature (Table 2).

**Electrochemical Properties of the Diazocine-Containing Polymer.** The cyclic voltammogram of 6,12-bis(4-fluorophenyl)-dibenzo[1,5]diazocine **1** is shown in Figure 8a as a model compound. Cathodic potential scan produced two reduction peaks at −0.76 and −1.23 V vs $Ag/Ag^+$, and the corresponding oxidation peaks at −0.61 and −1.19 V appeared under inert and basic conditions. The two hetero atoms of the diazocine unit contributed to the redox stability of the 8-membered ring. These two redox waves were reversible, and the peak-to-peak separation ($\Delta E$) of the second reduction wave was narrow (43 mV), which is typical behavior for the surface-confined redox species, suggesting the lower solubility of the reduced species after the first reduction process. These two redox couples were considered as the two-electron transfer process for the diazocine ring. Cyclic voltammograms of the diazocine-containing poly(arylene ether) exhibited stable redox behavior in a similar fashion to the model compound **1** (Figure 8b). The smaller peak current in the polymer **4a** compared with **1** suggested the smaller diffusion coefficient of the polymer analog. The UV−vis spectrum of the diazocine group in the reduced state under the applied potential at −1.4 V indicated an extended $\pi$-electron structure, which supported the boat- to planar-conformational change by a $2e^-$ reduction (Figure 8c). This process was reversible, and suggested the potential application of a diazocine unit for redox-driven molecular actuation. Cyclic voltammogram of the film **4a** in acetonitrile/THF (9/1) electrolyte solution exhibited similar redox behavior as the corresponding solution **4a**, and the peak-to-peak separation at −1.2 V was narrower (~ 38 mV), which also supported a surface-confined redox process of the film. Further electrochemical analysis and device fabrication will be reported in the future.

## Conclusions

Poly(arylene ether sulfone)s containing the diazocine unit (0, 20, 50, 80, and 100 mol %) were synthesized *via* step-growth polymerization. The resulting copolymers exhibited good solvent solubility, enhanced thermal ($T_{d10\%} = 500-550$ °C), and mechanical properties (tensile stress = 45−65 MPa), which were tunable with copolymer composition. The secondary ($\beta$-) transition appeared at *ca.* 28−40 °C, which was attributed to the larger free volume of the bulky diazocine unit and biphenyl motion. The conformation of the diazocine group was identified as boat-type using X-ray single crystallography and NMR spectroscopy at various temperatures. DIPSHIFT experiments indicated that the bulkier diazocine group undergoes relatively slower ring-flip motion compared to the smaller phenylene group. The cyclic voltammograms of diazocine-containing polysulfones showed two reversible reduction peaks under inert and basic conditions, followed by the conformational change, which proved its potential application as molecular actuator.

**Acknowledgment.** This work is supported by Solvay Advanced Polymers and the U.S. Army Research Laboratories Material Center of Excellence (MCOE). The authors acknowledge Prof. Thomas C. Ward for scientific discussion dealing with the characterization of mechanical properties. The authors acknowledges to Dr. Carla Slebodnick for X-ray single crystallographic analysis.

**Supporting Information Available:** Figures showing 2D NMR (COSY, HSQC and HMBC) spectra of diazocine-containing poly(arylene ether) **4a**, solution $^{13}$C NMR spectra for **4a**, **4c**, and **4e** with complete assignments based on 2D NMR experiments, DIPSHIFT NMR results for **4c** and **4e**, a theoretical simulation of the $^{13}$C$-$$^{1}$H dipolar coupling strength, and an Arrhenius plot for the $\beta$-transition of **4a** and **4e** and crystallographic information files (CIF). This material is available free of charge via the Internet at http://pubs.acs.org.

## References and Notes

(1) Wang, S.; McGrath, J. E. In *Synthetic Methods in Step-Growth Polymers*; Rogers, M. E., Long, T. E., Turner, S. R., Ed.; John Wiley & Sons: New York, 2003.

(2) Hickner, M. A.; Ghassemi, H.; Kim, Y.-S.; Einsla, B. R.; McGrath, J. E. *Chem. Rev.* **2004**, *104*, 4587–4611.

(3) Aitken, C. L.; McHattis, J. S.; Paul, D. R. *Macromolecules* **1992**, *25*, 2910–2922.

(4) David, L.; Girard, C.; Dolmazon, R.; Albrand, M.; Etienne, S. *Macromolecules* **1996**, *29*, 8343–8348.

(5) Fried, J. R.; Letton, A.; Welsh, W. J. *Polymer* **1990**, *31*, 1032–1037.

(6) Dumais, J. J.; Cholli, A. L.; Jelinski, L. W.; Hedrick, J. L.; McGrath, J. E. *Macromolecules* **1986**, *19*, 1884–1889.

(7) Quintana, I.; Arbe, A.; Colmenero, J.; Frick, B. *Macromolecules* **2005**, *38*, 3999–4013.

(8) Wu, S. *J. Appl. Polym. Sci.* **1992**, *46*, 619–624.

(9) Klug, C. A.; Wu, J. Xiao.; Yee, A. F.; Schaefer, J. *Macromolecules,* **1997**, *30*, 6302–6306.

(10) Chen, L. P.; Yee, A. F.; Goetz, J. M.; Schaefer, J. *Macromolecules* **1998**, *31*, 5371–5382.

(11) Schaefer, J.; Stejskal, E. O.; Buchdahl, R. *Macromolecules* **1977**, *10*, 384–405.

(12) Hedrick, J. L.; Yilgor, I.; Wilkes, G. L.; McGrath, J. E. *Polym. Bull.* **1985**, *13*, 201–208.

(13) Hedrick, J. L.; Yilgor, I.; Jurek, M.; Hedrick, J. C.; Wilkes, G. L.; McGrath, J. E. *Polymer* **1991**, *32*, 2020–2032.

(14) Wang, F.; Hickner, M.; Kim, Y. S.; Zawodzinski, T.; McGrath, J. E. *J. Membr. Sci.* **2002**, *197*, 231–242.

(15) Lin, Q.; Unal, S.; Fornof, A. R.; Yilgor, I.; Long, T. E. *Macromol. Chem. Phys.* **2006**, *207*, 576–586.

(16) Duncan, A. J.; Leo, D. J.; Long, T. E. *Polym. Prep.* **2007**, *48*, 853–854.

(17) Duncan, A. J.; Leo, D. J.; Long, T. E. *Macromolecules* **2008**, *41*, 7765−7775.

(18) Mao, M.; Das, S.; Turner, S. R. *Polymer* **2007**, *48*, 6241–6245.

(19) Osano, K.; Turner, S. R *J. Polym. Sci. A, Polym. Chem* **2008**, *46*, 958–969.

(20) Paquette, L. A. *Acc. Chem. Res.* **1993**, *26*, 57–62.

(21) Klarner, F.-G. *Angew. Chem., Int. Ed.* **2001**, *40*, 3977–3981.

(22) Spitler, E. L.; Johnson, C. A., II; Haley, M. M. *Chem. Rev.* **2006**, *106*, 5344–5386.

(23) Yu, Y.; Nakano, M.; Ikeda, T. *Nature* **2003**, *425*, 145–145.

(24) Yamada, M.; Kondo, M.; Mamiya, J.; Yu, Y.; Kinoshita, M.; Barrett, C. J.; Ikeda, T. *Angew. Chem., Int. Ed.* **2008**, *47*, 4986–4988.

(25) Yu, H.-H.; Xu, B.; Swager, T. M. *J. Am. Chem. Soc.* **2003**, *125*, 1142–1143.

(26) Casanovas, J.; Zanuy, D.; Aleman, C. *Angew. Chem., Int. Ed.* **2006**, *45*, 1103–1105.

(27) Kanazawa, H.; Higuchi, M.; Yamamoto, K. *J. Am. Chem. Soc.* **2006**, *127*, 16404–16405.

(28) Marsella, M. J.; Reid, R. J.; Estassi, S.; Wang, L.-S. *J. Am. Chem. Soc.* **2002**, *124*, 12507–12510.

(29) Marsella, M. J. *Acc. Chem. Res.* **2002**, *35*, 944–951.

(30) Webb, G. G.; Zilm, K. W. *J. Am. Chem. Soc.* **1989**, *111*, 2455–2463.

(31) Burum, D. P.; Bielecki, A. *J. Magn. Reson.* **1991**, *95*, 184–190.

(32) Sethi, N. K. *J. Magn. Reson.* **1991**, *94*, 352–361.

(33) Bielecki, A.; Kolbert, A. C.; de Groot, H. S. M.; Griffin, R. G.; Levitt, M. H. *Adv. Magn. Reson.* **1990**, *14*, 111.

(34) Benett, A. E.; Rienstra, C. M.; Auger, M.; Lakshmi, K. V.; Griffin, R. G. *J. Chem. Phys.* **1995**, *103*, 6951–6958.

(35) Margolis, J. M. *Engineering Plastics Handbook.* McGraw-Hill Companies, Inc.: New York, 2006.

MA802249A